JBC Papers in Press. Published on August 26, 2010 as Manuscript M110.164541
The latest version is at http://www.jbc.org/cgi/doi/10.1074/jbc.M110.164541

REQUIREMENT OF THE EPITHELIAL-SPECIFIC ETS TRANSCRIPTION FACTOR SPDEF FOR MUCOUS GLAND CELL FUNCTION IN THE GASTRIC ANTRUM

David Horst[1,#], Xuesong Gu[2,#], Manoj Bhasin[2], Quanli Yang[2], Michael Verzi[1], Dongxu Lin[2], Marie Joseph[2], Xiaobo Zhang[3], Wei Chen[4,5], Yi-Ping Li[4,5], Ramesh A Shivdasani[1,6], and Towia A Libermann[2]

From Department of Medical Oncology, Dana-Farber Cancer Institute and Department of Medicine, Harvard Medical School, Boston, Massachusetts, USA[1]; BIDMC Genomics and Proteomics Center and Div. of Interdisciplinary Medicine and Biotechnology, Beth Israel Deaconess Medical Center, and Department of Medicine, Harvard Medical School, Boston, Massachusetts, USA[2]; Gastrointestinal Unit and MGH Weight Center, Massachusetts General Hospital, Charlestown, Massachusetts, USA[3]; Department of Cytokine Biology, The Forsyth Institute, Boston, Massachusetts, USA[4]; Department of Oral Medicine, Infection and Immunity, Harvard School of Dental Medicine, Boston, Massachusetts, USA[5]. Both authors contributed equally[#].

Running head: Spdef is required for gastric antral mucous gland cell maturation

Address correspondence to: Towia A Libermann , 99 Brookline Ave, Boston, MA 02115. Fax: 617-667-0891; E-mail: tliberma@bidmc.harvard.edu **or** Ramesh A. Shivdasani, 44 Binney Street, Boston, MA 02215. Fax: 617-582-7198; E-mail: ramesh_shivdasani@dfci.harvard.edu

Mucus-secreting cells of the stomach epithelium provide a protective barrier against damage that might result from bacterial colonization or other stimuli. Impaired barrier function contributes to chronic inflammation and cancer. Knockout mice for the epithelium-specific transcription factor *Spdef* have defects in terminal differentiation of intestinal and bronchial secretory cells. We sought to determine the physiologic function of Spdef in the stomach, another site of significant levels of Spdef expression. We used in situ hybridization and immunohistochemistry to localize Spdef-expressing cells in the mouse stomach; targeted gene disruption to generate mice lacking Spdef; and histologic, immunologic and transcriptional profiling approaches to determine its requirements in stomach epithelial homeostasis. In wild-type mice Spdef RNA and protein are expressed predominantly in mucous gland cells of the antrum and in mucous neck cells of the glandular corpus. Within 1.5 years, nearly half of homozygous mutant mice developed profound mucosal hyperplasia of the gastric antrum. Sub-mucosal infiltration of inflammatory cells preceded antral hyperplasia by several weeks. Absence of Spdef impaired terminal maturation of antral mucous gland cells, as reflected in reduced expression of Muc6 and Tff2 and reduced numbers of secretory granules. Antral gene expression abnormalities overlapped significantly with those in *Spdef*$^{-/-}$ colon, including genes implicated in secretory granule traffic and functions. Spdef is required for terminal maturation of antral mucous gland cells to protect animals from gastric inflammation and resulting hyperplasia. These requirements parallel Spdef functions in secretory intestinal cells and suggest a common molecular mechanism for maturation of gastrointestinal secretory lineages.

The Ets protein family in humans and mice contains nearly 30 transcription factors. Loss of several family members in knockout mice reveals their critical requirement in embryogenesis, morphogenesis and cell differentiation (1-3). Deregulated expression or activation of Ets factors is also linked to various human cancers (4-5), highlighting their importance in disease. Ets proteins were first studied in detail in lymphocytes and neurons (6-7). Their role in epithelial cells gained attention after we and others identified four additional Ets factors: Elf3 (Ese1), Elf5 (Ese2), Ehf (Ese3) and Spdef (Pdef) (8-10). These factors are virtually restricted to epithelial cells but each shows a distinct tissue distribution, with further restriction to distinct cell subsets or differentiation stages (11), suggesting specialized roles in different lineages.

Spdef is unique among Ets proteins for its distinct DNA binding specificity and restricted expression in hormone-regulated prostate, mammary, endometrial and ovarian epithelia, salivary gland, trachea, lungs, and digestive tract (9,12). Spdef function has been studied in cancer cell migration and prostate, ovarian and breast cancer (13-16); its role in normal tissues is starting to emerge. Exposure to intratracheal allergens or IL-13 leads to excess mucus production as a result of Spdef-dependent goblet cell differentiation, whereas Spdef expression in transgenic bronchial epithelium causes goblet cell hyperplasia and mucus hypersecretion (17), defects related to human lung diseases. *Spdef*$^{-/-}$ mice show defective differentiation of pulmonary goblet cells and intestinal Paneth and goblet cells,

together with deregulation of secretory cell-specific genes (18-19).

After gastrointestinal (GI) mucosal progenitors commit to a particular cell fate, they undergo additional differentiation steps before acquiring the unique ability to absorb nutrients or secrete enzymes, mucus, acid, hormones or antimicrobial peptides. Combinations of cell type-specific and broadly expressed transcription factors regulate each step, as highlighted in recent reports of the roles of transcription factors Foxq1 and Mist1 in specific aspects of gastric foveolar (pit) and corpus mucous neck cells, respectively (20-21). In the intestine, *Spdef*$^{-/-}$ mice show reduced mucus production and low granule numbers in goblet and Paneth cells, respectively, implicating Spdef in terminal differentiation of these secretory cells (19,22). We generated an independent null allele for *Spdef* and here we report on the requirement for this epithelial Ets factor in the mammalian stomach. Antral mucosal hyperplasia develops in a significant fraction of *Spdef*$^{-/-}$ mice within 18 months in response to antecedent inflammation. We attribute this disorder to defects in maturation of mucous gland cells, which normally express high Spdef levels and in its absence show reduced numbers of secretory granules and reduced expression of Muc6 and Tff2. Thus, in addition to controlling maturation of intestinal goblet and Paneth cells, Spdef also regulates terminal differentiation of antral mucous gland cells. This activity is necessary for proper epithelial barrier function.

Experimental Procedures

Generation of mutant mice. *Spdef* clones were isolated from a 129/SvJ mouse genomic library (Stratagene). The targeting construct contained a 5-kb EcoRI/Hind III fragment and 2.6-kb HindIII/BglII fragment as the left and right homology arms, respectively, flanking a neomycin-resistance (Neo^R) cassette (Fig. 2A). For genotyping by Southern analysis, HindIII-digested genomic DNA was hybridized to a 700-bp probe from the 5' end of the *Spdef* locus (Fig. 2B) and SalI-digested DNA with a 500-bp 3' probe (data not shown). The targeting construct was electroporated into isogenic J1 embryonic stem (ES) cells and two targeted euploid ES cell clones were injected into C57BL/6 blastocysts. Heterozygote offspring of chimeric males were propagated in a continuous mating scheme on a hybrid 129/SvJ strain background and crossed to produce nullizygous mutants. Mice were handled according to institutional regulations. PCR genotyping used a common reverse primer and specific forward primers to amplify a 300-bp region in the wild type allele or a 720-bp region spanning *Spdef* and *Neo*^{R} sequences in the targeted allele (Fig. 2C, Suppl. Table 1). PCR conditions were 94.5°C for 45 s, 56°C for 45 s, and 72°C for 1 min for 35 cycles.

Gene expression analyses. Organs were excised after mouse euthanasia by CO_2 asphyxiation and stored at -80°C. RNA was isolated using TRIzol Reagent (Invitrogen), treated with DNaseI, and first-strand cDNA synthesized using oligo-(dT) primers. Quantitative real-time PCR was done using Sybr green (Roche) and a 7500 instrument (Applied Biosystems, Foster City, CA) with 40 cycles of amplification at 95°C (15 sec) and 60°C (1 min). Primers used for real-time PCR are listed in Suppl. Table 1. For transcriptional profiling, total RNA was hybridized to Affymetrix HT Mouse Genome 430A arrays (22,700 transcripts; Affymetrix, Santa Clara, CA) using protocols described previously (23) and the automated labeling protocol from Affymetrix. For in situ hybridization, tissues were rinsed in phosphate-buffered saline (PBS) and frozen in Tissue-TEK O.C.T. compound (Sakura, Torrance, CA). 9-µm sections were fixed in 4% paraformaldehyde in PBS for 2h at 4°C, washed in PBS, and treated thereafter as described previously. A hybridization probe complementary to mouse *Spdef* exons 3-5 was transcribed using DIG RNA labeling mix (Roche).

Histology, immunohistochemistry and Helicobacter testing. Tissues were fixed in 4% paraformaldehyde, dehydrated in ethanol and xylene, and embedded in paraffin. Sections were stained with hematoxylin and eosin, alcian blue (Sigma-Aldrich, St. Louis, MO), biotinylated *Griffonia Simplicifolia* lectin II (GSII, Vector, 1:100 for 1 h at room temperature) or Warthin-Starry (Marketlab, Grand Rapids, MI). For immunohistochemistry, antigens were retrieved in 10 mM Na citrate, pH 6, for 10 min in a pressure cooker (Biocare Medical, Concord, CA). Slides were blocked with 0.5% hydrogen peroxide in methanol for 20 min, followed by 5% fetal bovine serum in PBS for 30 min, then incubated with primary Ab overnight at 4°C, washed with PBS, and incubated with biotinylated species-specific secondary Ab (Vector, Burlingame, CA; 1:300) for 1 h at room temperature. Ab are listed in Suppl. Table 2. Staining was detected using the Vectastain Elite ABC kit (Vector) and diaminobenzidine as the substrate. Slides were counterstained with hematoxylin, dehydrated, mounted, and examined under an Olympus BX41 compound microscope. Testing for *Helicobacter*

species was done by PCR as previously described (24), using 150 ng genomic DNA as template and the primers listed in Suppl. Table 1. DNA was extracted from 5 wildtype and 5 *Spdef*$^{-/-}$ stomachs, and from stomach tissue known to be infected with *Helicobacter pylori*, using the DNeasy tissue kit (Qiagen, Hilden, Germany). DNA from cultured *H. pylori* served as an additional positive control.

Transmission electron microscopy. Mouse antra were isolated immediately after euthanasia, rinsed in PBS, fixed overnight (2.5% formaldehyde, 5 % glutaraldehyde, 0.06% picric acid 0.06% CaCl2, 0.1 M sodium cacodylate buffer, pH 7.4), post-fixed in OsO_4, and embedded in Epon 812 resin. Ultrathin sections were stained with uranyl acetate and lead citrate and examined on a JEOL 1200EX electron microscope at an accelerating voltage of 80 kV.

Quantitation and statistical analysis. Real-time RT-PCR results were first normalized to *Gapdh* mRNA levels and subsequently to levels of the corresponding transcript in wild-type littermates. At least 100 antral glands per group were counted for Ki67 staining, expressed as stained nuclei per gland. Secretory granules in mucous gland cells were counted on electron photomicrographs. Groups were compared using Student's t-test with $p<0.05$ regarded as statistically significant.

Expression microarray data quality was determined using the Simpleaffy package of Bioconductor (25) and outliers were checked using the dChip package (26). Arrays with <5% outlier probes were used to identify differential expression. Results were normalized using the RMA algorithm in Bioconductor, based on background correction, normalization, and summarization of signal values (25,27). Gene expression values were converted from $\log_2$ to linear scale for class comparison analysis and transcripts that achieved a mean change >1.3-fold and minimum change >1.2-fold between two groups were considered differentially expressed. An Unweighted Pair Group Method with Arithmetic-mean (UPGMA) tree was constructed using a hierarchical clustering technique and Pearson's correlation as the metric of similarity (28-29). The expression data matrix was row-normalized for each gene prior to application of average linkage clustering.

RESULTS

Spdef expression in mouse stomach. We mapped Spdef expression by quantitative real-time RT-PCR on RNA isolated from selected wild-type mouse organs. Among these tissues, *Spdef* expression was highest in the dorsal prostate, as expected (9), followed by the colon and stomach (Fig. 1A). Among the 3 major stomach compartments, *Spdef* expression is highest in the antrum, followed by the corpus, and absent in the forestomach (Fig. 1B). To corroborate these findings and to identify *Spdef*-expressing cell types, we performed immunohistochemistry with a well-characterized antibody (Ab) (17). Nuclear staining, as expected for a transcription factor, was undetectable in the forestomach (Suppl. Fig. 1A). In corpus glands, we observed nuclear staining in cells with a clear-foamy cytoplasm located in the neck region (Fig. 1C), the known site of mucous neck cells (30). Specific and consistently stronger nuclear staining appeared in similar clear-foamy cells at the base of antral glands (Fig. 1D), where mucous gland cells reside. Co-staining of Spdef-stained sections with Alcian Blue confirmed expression in antral mucous gland cells (Fig. 1E). We also observed high Spdef expression in Brunner's glands, a distinct compartment in the intestinal submucosa at the gastro-duodenal junction (Suppl. Fig. 1D). The morphology and properties of Brunner's glands are similar to those of gastric mucous neck cells (31).

In situ hybridization with a specific *Spdef* probe confirmed this expression pattern. Whereas low mRNA levels and background staining of chief (zymogenic) cells in the corpus confounded these efforts (data not shown), we consistently observed a specific signal at the base of antral glands with antisense but not with sense probes (Fig. 1F); riboprobe specificity was verified by absence of signal in *Spdef*$^{-/-}$ antrum (data not shown). Staining of hybridized sections with an Ab against the proliferation marker Ki67 localized *Spdef*-expressing cells in a distinct compartment of the antral mucosa, below the level of proliferating cells (Fig. 1F). These results together indicate that Spdef marks mucous cells of the neck and the basal region in gastric corpus and antral glands, respectively, with most prominent expression in the antrum.

Generation of Spdef$^{-/-}$ *mice.* We used homologous recombination in embryonic stem cells to create Spdef-null mice. Our targeting strategy (Fig. 2A) replaces a 5.1-kb fragment encompassing exons 2-5 with a PGK-Neo^R cassette. As the replaced exons encode the transactivation domain, Pointed domain, and most of the Ets DNA-binding domain (DBD), the resulting mice are predicted to carry a functionally null *Spdef* allele. RT-PCR analysis confirmed loss of sequences originating in exons 2-3 (Suppl. Fig. 1B). We also verified absence of Spdef by

immunostaining (Suppl. Fig. 1C-E) and by in situ hybridization using a probe that corresponds to the deleted exons (data not shown). Heterozygote crosses yielded all three expected genotypes (Fig. 2C). Most *Spdef*$^{-/-}$ mice were viable at birth, although they appeared in ratios slightly lower than expected from heterozygote matings (18% instead of 25%, n=162, p=0.16, Suppl. Table 3). As discussed below, intestinal gene expression profiles in our *Spdef*$^{-/-}$ mouse strain overlapped considerably with those reported with another, independent null allele (19).

Polypoid antral hyperplasia in the Spdef$^{-/-}$ *stomach.* Although the stomachs of *Spdef*$^{-/-}$ mice did not differ overtly from those of their wild-type littermates in the first 2 months of life, profound thickening of the antral stomach was evident on gross inspection of a significant fraction of homozygote mutant animals (40.9% at ≥4 months age) at necropsy (Fig. 3A). By histology, mice with such antral thickening showed marked polypoid hyperplasia, with impressive expansion of the epithelium and dilated, elongated and tortuous foveolae (compare Figs. 3C and 3B). Ki67 staining revealed an expanded zone of proliferating antral epithelial cells, located predominantly in the mid-gland (Fig. 3D), although the spectrum of variation included samples with proliferating cells present almost throughout the antral epithelium (Suppl. Figure 2C). The hyperplastic mucosa was separated by myofibroblast bands containing cells that express α-smooth muscle actin (Fig. 3E). Some mutant antra harbored scattered epithelial cysts (Suppl. Fig. 2A) or areas with tubular or cribriform growth (Suppl. Fig. 2B). No signs of severe dysplasia, carcinoma *in situ* or invasive carcinoma were evident, even at 18 months of age (n=3). Hyplerplastic glands expressed the foveolar pit cell marker Muc5ac mainly near the luminal surface (Fig. 3E) and did not stain for the chief cell marker Gastric Intrinsic Factor (Gif), the parietal cell marker Atp4b or the intestine-specific protein Cdx2 (Suppl. Fig. 2D-F), indicating absence of tissue heterotopia or metaplasia. No mice showed corpus mucosal abnormalities, including glandular atrophy. In summary, about half of *Spdef*$^{-/-}$ adult mice developed severe polypoid hyperplasia of the gastric antrum over a 1.5-year period of observation.

Inflammation precedes antral hyperplasia in Spdef$^{-/-}$ *mice.* Because antral mucosal hyperplasia occurred in *Spdef*$^{-/-}$ mice with incomplete penetrance and increased in frequency with age, we considered it less likely that the changes were direct effects of Spdef loss and more likely that they represented a secondary response. Acute and chronic gastritis are common causes of reactive and neoplastic stomach mucosal hyperplasia in mice and humans (32-33), prompting us to assess inflammation in the *Spdef*$^{-/-}$ stomach mucosa. Moderate to severe inflammation was evident in nearly 90% of mutant mice after 4 months, in the form of dense leukocytic infiltrates in a band-like pattern among the bases of the antral glands (Fig. 4A). This feature was present even in the absence of epithelial hyperplasia and certainly earlier (Fig. 4A) but absent from wild-type littermates. The characteristic nuclear ring shape permitted recognition of large numbers of neutrophils, and immunostaining confirmed a predominance of myeloperoxidase-expressing granulocytes, with few CD3^{+} T or B220^{+} B lymphocytes (Fig. 4B), indicating acute inflammation. In cases with accompanying epithelial hyperplasia, typically in older animals, we detected mixed inflammatory infiltrates in the lamina propria, with formation of sub-mucosal lymphoid follicles (Fig. 4C). Inflammation was usually absent from the gastric corpus (Suppl. Fig. 3A) in the absence of antral hyperplasia but often evident at the corpus-antral junction when antral hyperplasia was present (Suppl. Fig. 3B); less dense leukocytic infiltrates were also apparent in the duodenal sub-mucosa in these cases. Thus, inflammation centered on the gastric antrum, with some rostral and caudal extension. Approximately half of *Spdef*$^{-/-}$ mice euthanized for analysis between 4 and 18 months showed antral inflammation without hyperplasia but we never observed antral hyperplasia without accompanying inflammation. We therefore reason that inflammation precedes a reactive hyperplasia of the antral mucosa in *Spdef*$^{-/-}$ mice. Although *Helicobacter* infection could have contributed in principle to the gastric antral inflammation, neither histochemistry nor a PCR-based assay for *Helicobacter* DNA uncovered evidence of *Helicobacter* infection (Suppl. Fig. 3C-D). Thus, an underlying extrinsic stimulus for antral inflammation is unclear.

Spdef is required for proper maturation of mucous gland cells. Unlike the gastric corpus, which houses parietal and zymogenic cells, the antral epithelium carries a limited number of cell types (Fig. 1D). We analyzed antra from *Spdef*$^{-/-}$ and littermate control mice between 1 and 2 months in age, before onset of overt inflammation. Ki67 staining revealed equal proportions of proliferating cells in the mutant and control antra, with normal location of replicating cells above the gland base. Staining for Muc5ac and gastrin indicated normal maturation of foveolar pit and gastrin-producing G cells, respectively (Suppl. Fig. 4A-C). Because Spdef

expression is confined to mucous gland cells, we hypothesized that defects in this population may be responsible for the inflammatory prodrome and eventual mucosal hyperplasia in null mice. To test this hypothesis, we first used reverse transcription real-time PCR and found that *Muc6* and *Tff2* mRNAs, two specific markers of antral mucous gland cells (34-35), were significantly reduced in *Spdef*$^{-/-}$ mouse stomach (Fig. 5A); Tff2 immunohistochemistry confirmed the result (Fig. 5B). N-acetyl-D-glucosaminyl moieties on glycoproteins are specifically found in antral mucous gland cells (36) and staining for *Griffonia simplicifolia* lectin GS-II, which selectively binds this moiety, was also reduced in *Spdef*$^{-/-}$ antra (Fig. 5C). We characterized the apparent maturation defects further by transmission electron microscopy. Wild-type antral mucous gland cells carried multiple mucus granules in the apex, poised for secretion into the foveolar lumen (Fig. 5D). Granule numbers were significantly reduced in *Spdef*$^{-/-}$ antra (Fig. 5D-E) and appeared immature in their frequent lack of the typical composite feature of compartments with high and low electron density (Fig. 5F). Thus, antral mucous gland cells are produced in the absence of Spdef but have significant deficiencies in their secreted products. Ultrastructural analysis further reveals a paucity of secretory granules with a structural defect.

Spdef regulates a distinct set of stomach genes. To investigate the transcriptional consequences of Spdef loss, we profiled gene expression in the gastric antrum at 6 weeks of age, when morphologic or inflammatory changes are absent. Figure 6A shows the 50 genes most significantly deregulated in *Spdef*$^{-/-}$ antra. Real-time RT-PCR confirmed sample results (Fig. 6B), such as for *Thrsp*, a gene that is also strongly downregulated in gastric antral hyperplasia-prone *Tff2*$^{-/-}$ mice (37). Among 713 genes affected in the antrum, 122 were also dysregulated in the colon, representing a notable overlap (p=0.0001, Fig. 6C, Suppl. Fig. 5). Intestinal expression analysis of a different *Spdef*$^{-/-}$ strain had revealed reduced expression of genes that may be necessary for Paneth and goblet cell maturation (19); our antral and intestinal expression profiles overlapped with the published list of 25 such genes. Six of these transcripts (*Creb3l4*, *Ccl6*, *Ccl9*, *Hgfac*, *Rap1gap*, *Es1*) are reduced in antrum and small intestine, and 5 genes (*Tpsg1*, *Spink4*, *1810030J14Rik*, *Mmp7*, *Foxa3*) only in the intestine in our *Spdef*$^{-/-}$ strain (Suppl. Tables 4 and 5), suggesting that each mouse line reflects *bona fide* consequences of Spdef loss. mRNA profiling (Fig. 6A) and RT-PCR analysis (Fig. 6D) of stomach and colon from our *Spdef*$^{-/-}$ mice confirmed reduced levels of *Creb3l4* and *Mlph*, two genes whose expression correlates most closely with *Spdef* across multiple tissues (Fig. 6D). Thus, a subset of Spdef-dependent genes, exemplified by such factors, represents an apparently common program in functional maturation of gastric and intestinal secretory cells.

DISCUSSION

Distinct regions in the mammalian stomach are distinguished by the presence of highly specialized glandular epithelial cells such as acid-secreting parietal and zymogenic chief cells in the corpus, and gastrin-producing endocrine and mucous gland cells in the antrum. In addition to secretory functions, the gastric mucosa also forms a barrier against damage from ingested food and microbes. All epithelial cell lineages derive from a common progenitor but few transcriptional regulators of cell fate determination and terminal differentiation have been identified. Significant expression of the epithelial Ets protein Spdef in the distal stomach suggested the possibility of such a role.

Spdef is expressed in mucous neck and gland cells of the corpus and antrum, respectively. We show that *Spdef* gene deletion leads to reduced expression of known protective factors like Muc6 and Tff2 and to significantly reduced numbers and defects in secretory granules in antral mucous gland cells. These observations parallel recent findings in the intestine, where Spdef specifically regulates maturation of goblet and Paneth cells (19). Taken together with the observation that Spdef controls terminal differentiation of goblet cells in the lung (18) and of luminal epithelial cells in the prostate (Gu et al., manuscript in preparation), this transcription factor appears to enable maturation of specialized secretory cells in several organs. Of particular interest in this light are the phenotypic similarities between intestinal goblet and gastric antral mucous gland cells, each of which matures incompletely in the absence of Spdef. These two cell types represent a subset of the highly specialized mucin-producing cells that populate the digestive mucosa and produce acidic mucins necessary to protect the epithelium (38-39). Needs for particular mucins vary along the gastrointestinal tract and mucin-producing cells have evolved to meet those needs. Goblet cell numbers increase steadily from the duodenum, where they are sparse, to the colon, where they constitute the majority, and differ materially from the dominant mucinous cells in the stomach, pit cells, which produce alkaline mucins. Spdef-

dependent mucous cells in the gastric antrum are distinctive but poorly characterized. Their morphology, location and staining properties place them closest to the network of submucosal secretory cells in duodenal Brunner's glands (31), another poorly characterized population which also shows Spdef expression. The shared dependence on Spdef suggests that, although antral mucous and intestinal goblet cells serve different, region-specific functions, they may have evolved from a common cellular ancestor that first used Spdef for coordinate regulation of secretory granule products.

The secretory cell defects did not affect epithelial proliferation or other neighboring cell types in young animals. Over time, however, compromised mucous cell maturation led to antral gastritis in most *Spdef*$^{-/-}$ mice, with polypoid antral hyplerplasia, likely reactive, ensuing in about half the cases. These findings imply that Spdef-mediated mucous gland cell maturation is required for protective barrier function. *Spdef*$^{-/-}$ mucous gland cells showed reduced expression of Tff2, a protease-resistant peptide that is co-secreted with mucus and thought to help in oligomerization of mucin polysaccharides to form a protective viscous coat (35,40). Tff2-null mice are prone to epithelial hyperplasia and dysplasia upon *H. pylori* infection, whereas supplementary administration of Tff2 accelerates healing of gastric mucosal ulcers (41). Thus, Spdef may exert protection in part through control of Tff2 expression. We also observed reduced expression of Muc6 and reduced staining with GS-II lectin in antral mucous gland cells, suggesting a broad role for Spdef in completing the maturation necessary to produce an effective epithelial barrier.

Gene expression analysis provided additional clues. Both *Spdef*$^{-/-}$ antrum and intestine have reduced levels of Creb3l4, an endoplasmic reticulum- associated transcription factor of unknown function (42). *Creb3l4* is the transcript most closely correlated to *Spdef* across numerous expression datasets (unpublished results), followed by *Mlph*. *Mlph* is expressed highest in Spdef^{+} epithelia and belongs to a family that regulates secretory granules (43-44), suggesting a potential role in the *Spdef*$^{-/-}$ antral secretory defects. *Dmbt1*, one of the genes most increased in *Spdef*$^{-/-}$ antrum, is highly expressed in lung, intestinal, salivary and mammary gland epithelia and in the neck region of gastric glands; its levels increase in response to inflammation and decrease in terminally differentiated epithelia (45). Thus, increased Dmbt1 may contribute to incomplete mucous cell differentiation in the *Spdef*$^{-/-}$ antrum. Additional genes with diminished expression in the intestine of an independent *Spdef*$^{-/-}$ strain, including *Hgfac, Ccl6*, *Ccl9*, *Rap1gap* and *Es1* (19), are also reduced in the antrum, and the colon and antrum share 122 dysregulated genes, indicating that candidate Spdef target genes are common to several types of secretory gut epithelia.

REFERENCES

1. Barton, K., Muthusamy, N., Fischer, C., Ting, C. N., Walunas, T. L., Lanier, L. L., and Leiden, J. M. (1998) *Immunity* **9**, 555-563
2. Bartel, F. O., Higuchi, T., and Spyropoulos, D. D. (2000) *Oncogene* **19**, 6443-6454
3. Hendricks, T. J., Fyodorov, D. V., Wegman, L. J., Lelutiu, N. B., Pehek, E. A., Yamamoto, B., Silver, J., Weeber, E. J., Sweatt, J. D., and Deneris, E. S. (2003) *Neuron* **37**, 233-247
4. Delattre, O., Zucman, J., Plougastel, B., Desmaze, C., Melot, T., Peter, M., Kovar, H., Joubert, I., de Jong, P., Rouleau, G., and et al. (1992) *Nature* **359**, 162-165
5. Golub, T. R., Barker, G. F., Lovett, M., and Gilliland, D. G. (1994) *Cell* **77**, 307-316
6. Lin, J. H., Saito, T., Anderson, D. J., Lance-Jones, C., Jessell, T. M., and Arber, S. (1998) *Cell* **95**, 393-407
7. Akbarali, Y., Oettgen, P., Boltax, J., and Libermann, T. A. (1996) *J Biol Chem* **271**, 26007-26012
8. Oettgen, P., Alani, R. M., Barcinski, M. A., Brown, L., Akbarali, Y., Boltax, J., Kunsch, C., Munger, K., and Libermann, T. A. (1997) *Mol Cell Biol* **17**, 4419-4433
9. Oettgen, P., Finger, E., Sun, Z., Akbarali, Y., Thamrongsak, U., Boltax, J., Grall, F., Dube, A., Weiss, A., Brown, L., Quinn, G., Kas, K., Endress, G., Kunsch, C., and Libermann, T. A. (2000) *J Biol Chem* **275**, 1216-1225
10. Kas, K., Finger, E., Grall, F., Gu, X., Akbarali, Y., Boltax, J., Weiss, A., Oettgen, P., Kapeller, R., and Libermann, T. A. (2000) *J Biol Chem* **275**, 2986-2998
11. Oettgen, P., Kas, K., Dube, A., Gu, X., Grall, F., Thamrongsak, U., Akbarali, Y., Finger, E., Boltax, J., Endress, G., Munger, K., Kunsch, C., and Libermann, T. A. (1999) *J Biol Chem* **274**, 29439-29452

12. Yamada, N., Tamai, Y., Miyamoto, H., and Nozaki, M. (2000) *Gene* **241**, 267-274
13. Feldman, R. J., Sementchenko, V. I., Gayed, M., Fraig, M. M., and Watson, D. K. (2003) *Cancer Res* **63**, 4626-4631
14. Gunawardane, R. N., Sgroi, D. C., Wrobel, C. N., Koh, E., Daley, G. Q., and Brugge, J. S. (2005) *Cancer Res* **65**, 11572-11580
15. Gu, X., Zerbini, L. F., Otu, H. H., Bhasin, M., Yang, Q., Joseph, M. G., Grall, F., Onatunde, T., Correa, R. G., and Libermann, T. A. (2007) *Cancer Res* **67**, 4219-4226
16. Ghadersohi, A., Odunsi, K., Zhang, S., Azrak, R. G., Bundy, B. N., Manjili, M. H., and Li, F. (2008) *Int J Cancer* **123**, 1376-1384
17. Park, K. S., Korfhagen, T. R., Bruno, M. D., Kitzmiller, J. A., Wan, H., Wert, S. E., Khurana Hershey, G. K., Chen, G., and Whitsett, J. A. (2007) *J Clin Invest* **117**, 978-988
18. Chen, G., Korfhagen, T. R., Xu, Y., Kitzmiller, J., Wert, S. E., Maeda, Y., Gregorieff, A., Clevers, H., and Whitsett, J. A. (2009) *J Clin Invest* **119**, 2914-2924
19. Gregorieff, A., Stange, D. E., Kujala, P., Begthel, H., van den Born, M., Korving, J., Peters, P. J., and Clevers, H. (2009) *Gastroenterology* **137**, 1333-1345 e1331-1333
20. Ramsey, V. G., Doherty, J. M., Chen, C. C., Stappenbeck, T. S., Konieczny, S. F., and Mills, J. C. (2007) *Development* **134**, 211-222
21. Verzi, M. P., Khan, A. H., Ito, S., and Shivdasani, R. A. (2008) *Gastroenterology* **135**, 591-600
22. Noah, T. K., Kazanjian, A., Whitsett, J., and Shroyer, N. F. (2010) *Exp Cell Res* **316**, 452-465
23. Jones, J., Otu, H., Spentzos, D., Kolia, S., Inan, M., Beecken, W. D., Fellbaum, C., Gu, X., Joseph, M., Pantuck, A. J., Jonas, D., and Libermann, T. A. (2005) *Clin Cancer Res* **11**, 5730-5739
24. Beckwith, C. S., Franklin, C. L., Hook, R. R., Jr., Besch-Williford, C. L., and Riley, L. K. (1997) *J Clin Microbiol* **35**, 1620-1623
25. Gentleman, R. C., Carey, V. J., Bates, D. M., Bolstad, B., Dettling, M., Dudoit, S., Ellis, B., Gautier, L., Ge, Y., Gentry, J., Hornik, K., Hothorn, T., Huber, W., Iacus, S., Irizarry, R., Leisch, F., Li, C., Maechler, M., Rossini, A. J., Sawitzki, G., Smith, C., Smyth, G., Tierney, L., Yang, J. Y., and Zhang, J. (2004) *Genome Biol* **5**, R80
26. Li, C., and Hung Wong, W. (2001) *Genome Biol* **2**, RESEARCH0032
27. Irizarry, R. A., Hobbs, B., Collin, F., Beazer-Barclay, Y. D., Antonellis, K. J., Scherf, U., and Speed, T. P. (2003) *Biostatistics* **4**, 249-264
28. Sneath, P. H. A. (1973) *Numerical taxonomy; the principles and practice of numerical classification*, W. H. Freeman, San Francisco, CA
29. Hartigan, J. A. (1975) *Clustering algorithms*, Wiley, New York,
30. Lee, E. R., Trasler, J., Dwivedi, S., and Leblond, C. P. (1982) *Am J Anat* **164**, 187-207
31. Hughes, N. R., Bhathal, P. S., and Francis, D. M. (1994) *J Clin Pathol* **47**, 53-57
32. Jain, R., and Chetty, R. (2009) *Dig Dis Sci* **54**, 1839-1846
33. Judd, L. M., Alderman, B. M., Howlett, M., Shulkes, A., Dow, C., Moverley, J., Grail, D., Jenkins, B. J., Ernst, M., and Giraud, A. S. (2004) *Gastroenterology* **126**, 196-207
34. Ho, S. B., Roberton, A. M., Shekels, L. L., Lyftogt, C. T., Niehans, G. A., and Toribara, N. W. (1995) *Gastroenterology* **109**, 735-747
35. Jeffrey, G. P., Oates, P. S., Wang, T. C., Babyatsky, M. W., and Brand, S. J. (1994) *Gastroenterology* **106**, 336-345
36. Falk, P., Roth, K. A., and Gordon, J. I. (1994) *Am J Physiol* **266**, G987-1003
37. Baus-Loncar, M., Schmid, J., Lalani el, N., Rosewell, I., Goodlad, R. A., Stamp, G. W., Blin, N., and Kayademir, T. (2005) *Cell Physiol Biochem* **16**, 31-42
38. Lamont, J. T. (1992) *Ann N Y Acad Sci* **664**, 190-201
39. Yamazaki, Y., Ueda, T., Kohli, Y., Fujiki, N., Imamura, Y., and Fukuda, M. (1992) *Eur J Histochem* **36**, 161-176
40. Kindon, H., Pothoulakis, C., Thim, L., Lynch-Devaney, K., and Podolsky, D. K. (1995) *Gastroenterology* **109**, 516-523
41. Poulsen, S. S., Thulesen, J., Christensen, L., Nexo, E., and Thim, L. (1999) *Gut* **45**, 516-522
42. Labrie, C., Lessard, J., Ben Aicha, S., Savard, M. P., Pelletier, M., Fournier, A., Lavergne, E., and Calvo, E. (2008) *J Steroid Biochem Mol Biol* **108**, 237-244
43. Matesic, L. E., Yip, R., Reuss, A. E., Swing, D. A., O'Sullivan, T. N., Fletcher, C. F., Copeland, N. G., and Jenkins, N. A. (2001) *Proc Natl Acad Sci U S A* **98**, 10238-10243

44. Kuroda, T. S., Ariga, H., and Fukuda, M. (2003) *Mol Cell Biol* **23**, 5245-5255
45. Kang, W., and Reid, K. B. (2003) *FEBS Lett* **540**, 21-25

FOOTNOTES

We are grateful to Jeff Whitsett for sharing Spdef Ab, David Alpers for sharing Gif Ab, Nick Wright for sharing Tff2 Ab, Sarah Keates for providing *Helicobacter* DNA, and Jens Neumann for providing *Helicobacter* infected tissue. Supported by National Institutes of Health grants CA85467 (to TAL), DK081113 (to RAS) and AR44741 (to YPL), a Prostate Cancer Foundation award (to XG), and a fellowship from the Deutsche Forschungsgemeinschaft (to DH). Correspondence may be addressed to TAL (tliberma@bidmc.harvard.edu) or RAS (ramesh_shivdasani@dfci.harvard.edu). Gene expression data are accessible through GEO Series accession number GSE20299.

FIGURE LEGENDS

Fig. 1. Expression of Spdef in the mouse stomach. (**A**) Quantitative real-time RT-PCR from triplicate experiments comparing *Spdef* expression in different mouse organs, including the stomach. (**B**) The distinct stomach compartments (represented schematically) show different *Spdef* expression levels by quantitative real-time RT-PCR, with highest expression in the antrum. (**C, D**) Low- and high-power magnifications of Spdef immunohistochemistry in the gastric corpus shows nuclear staining of cells in the mid-gland compartment (**C**, arrow) where mucous neck cells reside, and at the base of antral foveolar crypts (**D**, arrow) where mucous gland cells reside. Images to the right are higher magnifications of the middle panels. Schematic drawings of corpus and antral glands are given for orientation; *scale bars*, 100 μm middle panels, 25 μm right panels. (**E**) Co-localization of nuclear Spdef staining (arrow) with Alcian blue staining in the gastric antrum; *scale bar*, 25 μm. (**F**) *Spdef* in situ hybridization confirms expression at the base of antral glands. Co-staining with Ki67 shows that Spdef is expressed below the proliferative compartment (delineated by dashed line) of antral glands; *scale bar*, 100 μm.

Fig. 2. Targeted mutation of *Spdef* in ES cells and mice. (**A**) The targeting vector carried a 5-kb EcoRI/Hind III fragment as the left homology arm and a 2.6-kb HindIII/Bgl II fragment as the right arm, flanking a Neo^R cassette. In the targeted allele, 5.1 kb of *Spdef* sequence spanning exons 2-5 was replaced with the PGK-Neo^R cassette. (**B**) Southern blot analysis of ES cell DNA. Lane 2, 3, 4 and 7 show $Spdef^{+/-}$ (mut) clones, with the expected band sizes of 8.2 kb and 10.4 kb with a 5' probe. Lanes 1 and 6 show $Spdef^{+/+}$ (wt) genotype with the expected band size of 8.2 kb. (**C**) Genotype analysis of mouse tail DNA by PCR, showing recovery of all 3 expected genotypes from heterozygote crosses.

Fig. 3. Polypoid antral hyperplasia in $Spdef^{-/-}$ mice. (**A**) Macroscopic appearance of antral mucosal thickening and frequency of antral hyplerplasia in $Spdef^{-/-}$ mice; *scale bar* 5 mm. (**B-E**) Compared to normal wild-type antra (**B**), histology of the lesions reveals elongated, tortuous foveolae (**C**) with expanded proliferative zones (**D**, Ki67 staining) and separation of glands by smooth muscle actin (Sma)-expressing connective tissue bands (**E**, arrow). Foveolar pit cell differentiation is preserved, as indicated by apical Muc5ac staining (**E**, arrows). Insets show higher magnifications of the boxed areas. *Scale bars*, 100 μm (B), 250 μm (C).

Fig. 4. Gastric antral inflammation in *Spdef* mutant mice. (**A**, **B**) Antral inflammation without mucosal hyperplasia. (**A**) Band-like (arrows) inflammatory infiltrates at the foveolar crypt base of the gastric antrum and frequency of inflammation (table). (**B**) Higher magnification of inflammatory cells (arrow) surrounding gland bases (arrowhead). Immunostaining identified predominantly granulocytes (myeloperoxidase, MPO) but few T (CD3, arrow) or B cells (B220, arrow). (**C**) Inflammation coincident with mucosal hyplerplasia showed mucosal infiltration by granulocytes (MPO, arrows), T (CD3, arrows) and B lymphocytes (left panel of B220 staining, arrow), and submucosal lymphoid aggregates (right panel of B220 staining). *Scale bars*, 100 μm (A), 50 μm (B), 250 μm (C-E).

Fig. 5. Defects in mucous gland cell maturation in $Spdef^{-/-}$ antra. (**A**) Significant ($p<0.001$) decrease of *Muc6* and *Tff2* mRNAs in $Spdef^{-/-}$ (KO) antra compared to the wild-type (WT), as determined by quantitative RT-PCR. (**B, C**) Strongly reduced staining for Tff2 (**B**) and GS-II lectin (**C**) in $Spdef^{-/-}$ antral mucous gland cells compared to WT littermates. (**D, E**) Significantly reduced numbers of secretory

granules in antral mucous gland cells of *Spdef*$^{-/-}$ (KO) mice compared to wild-type (WT) littermates. Granule counts (**E**) show data from 3 independent mouse pairs. (**F**) Immature appearance of granules in *Spdef*$^{-/-}$ antral mucous gland cells, with common absence of the wild-type (WT) feature of a composite of electron-dense and less dense compartments. *Scale bars*, 50 μm (B, C), 2 μm (D), 0.5 μm (F).

Fig. 6. Gene expression analysis of gastric antrum and colon. (**A**) Heat map showing the top 50 down- and up-regulated transcipts in *Spdef*$^{-/-}$ (KO) gastric antrum relative to wild type (WT) and *Spdef*$^{+/-}$ (HET) mice. Columns represent samples and rows represent genes. Expression is represented in a pseudocolor scale (-2 to 2), with red denoting high and green denoting low relative expression. (**B**) qRT-PCR validation of transcripts affected by Spdef absence. Real-time PCR analysis of *Pthlh*, *Dmbt1*, *Thrsp*, *Cfd*, and *Adipoq* in antrum from 8-week old mice of the 3 genotypes. Each mRNA was normalized to *glyceradehyde-3-phosphate dehydrogenase* (*Gapdh*) levels. (**C**) Venn diagrams highlighting the overlap in dysregulation of antral and colonic genes in *Spdef*$^{-/-}$ and WT mice. The numbers refer to transcripts showing significant differential expression. (**D**) Real-time RT-PCR results of *Spdef*, *Creb3l4* and *Mlph* expression in antrum and colon.

Figure 1

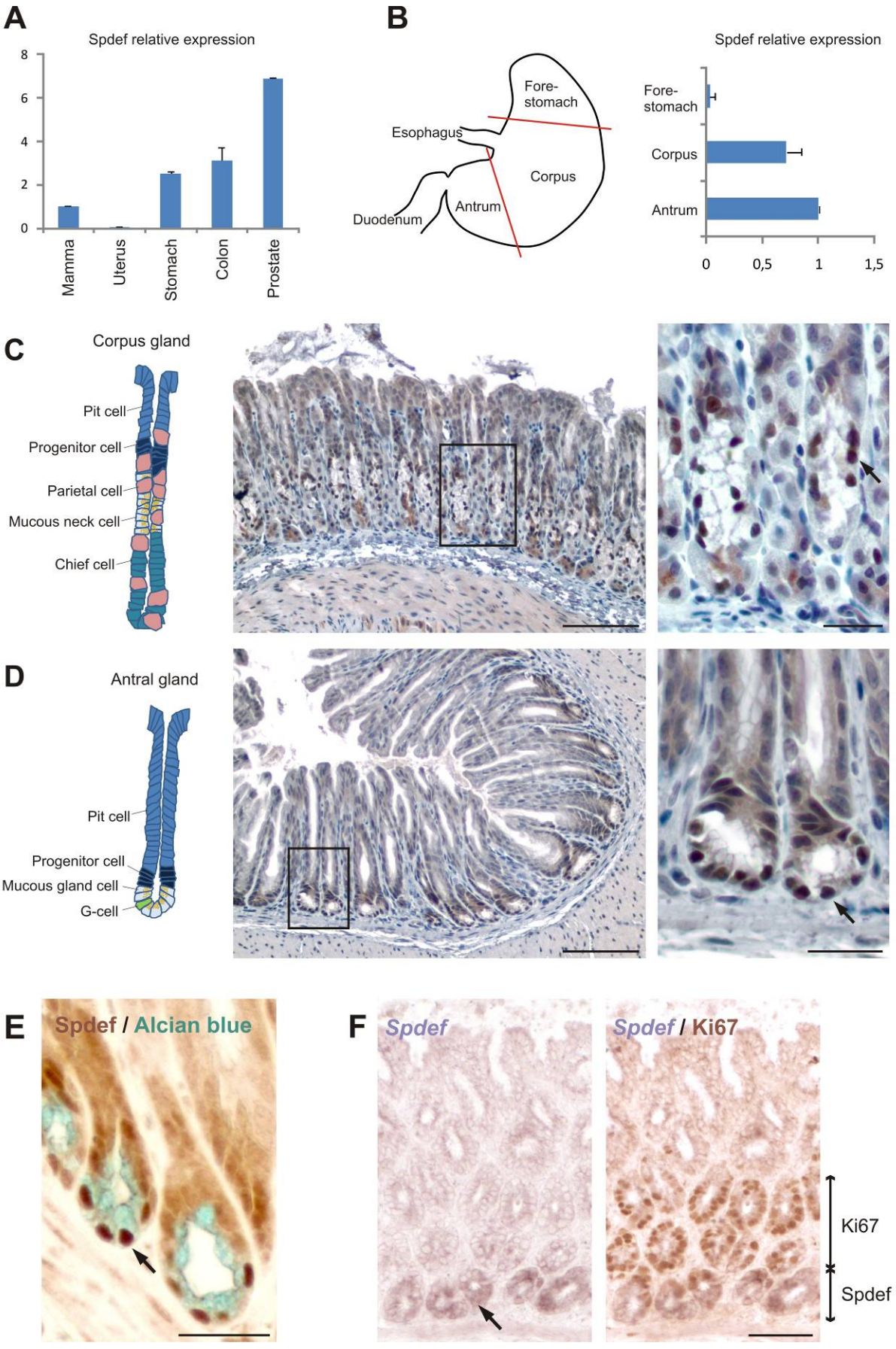

Figure 2

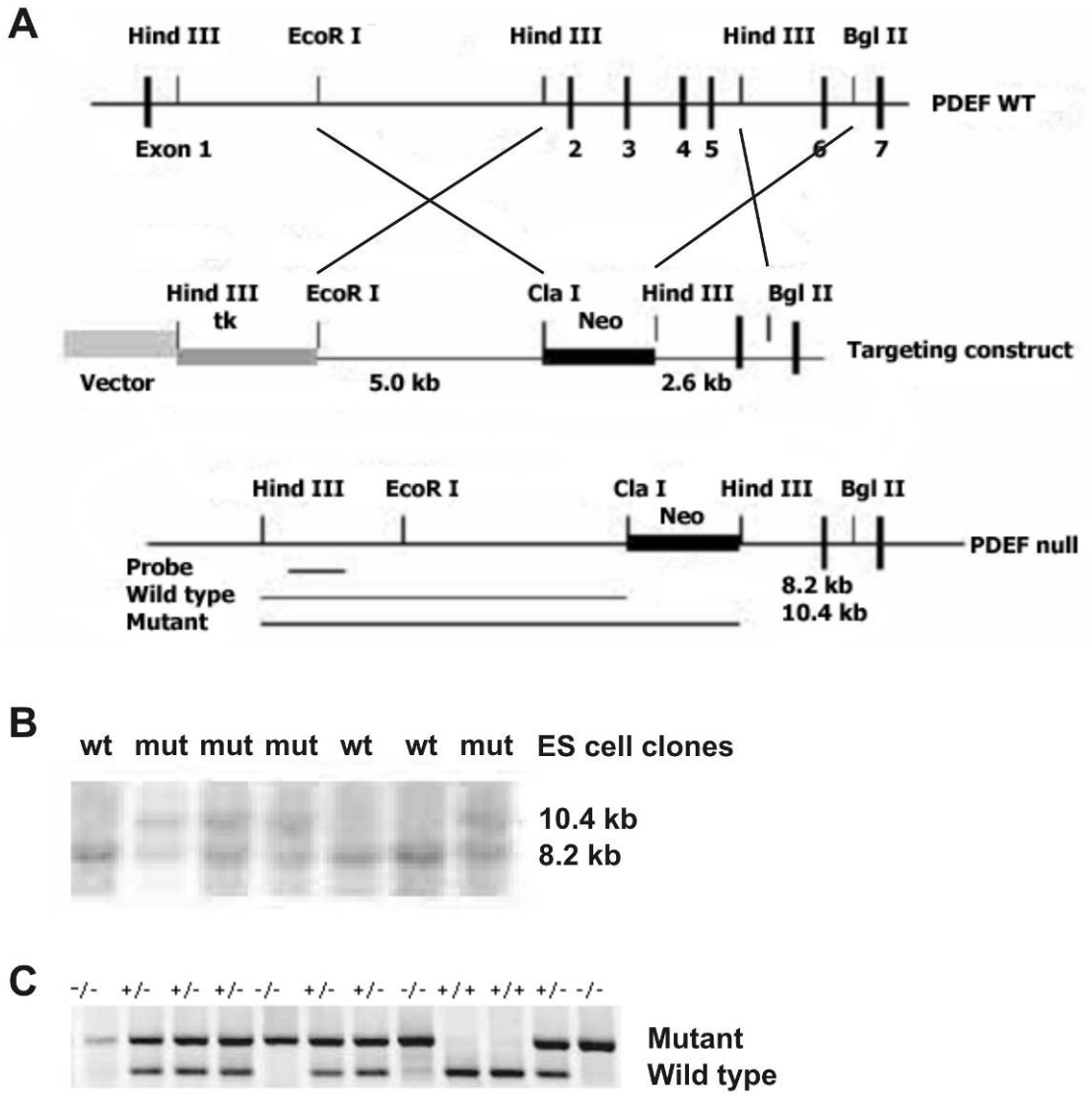

Figure 3

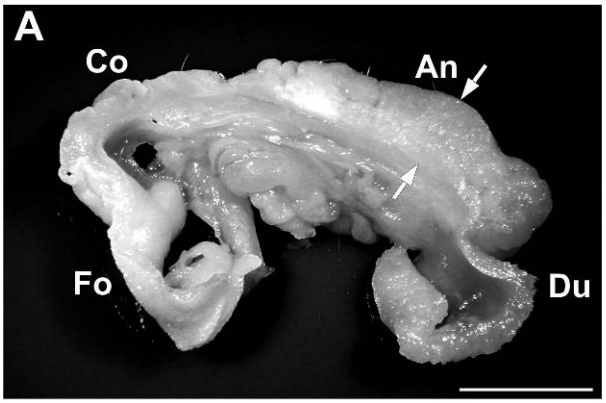

Mucosal hyperplasia	Age group 1-2 months (n=12)	4-6 months (n=8)	≥9 months (n=14)
absent	100%	62.5%	57.1%
present	0%	37.5%	42.9%

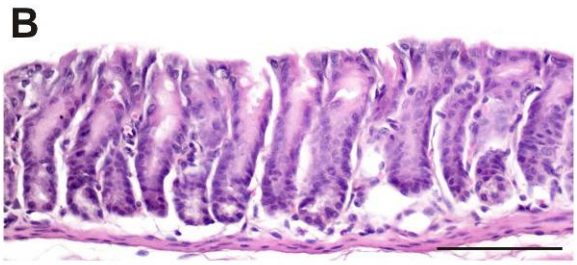

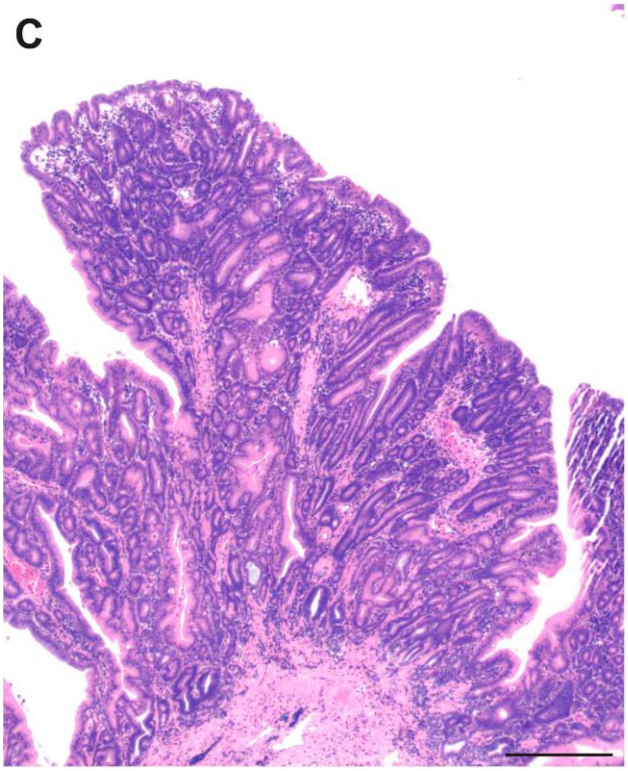

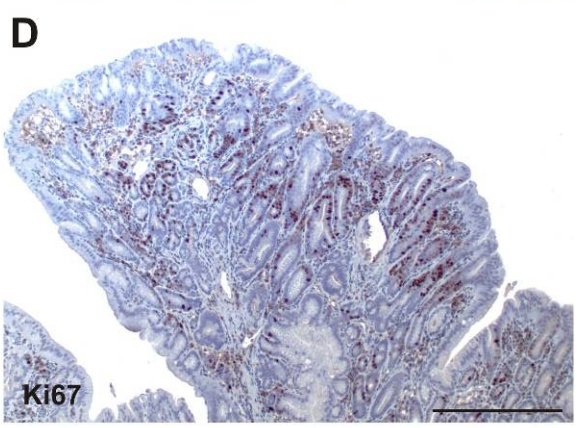

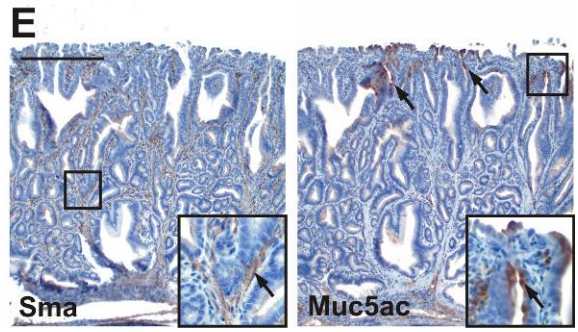

Figure 4

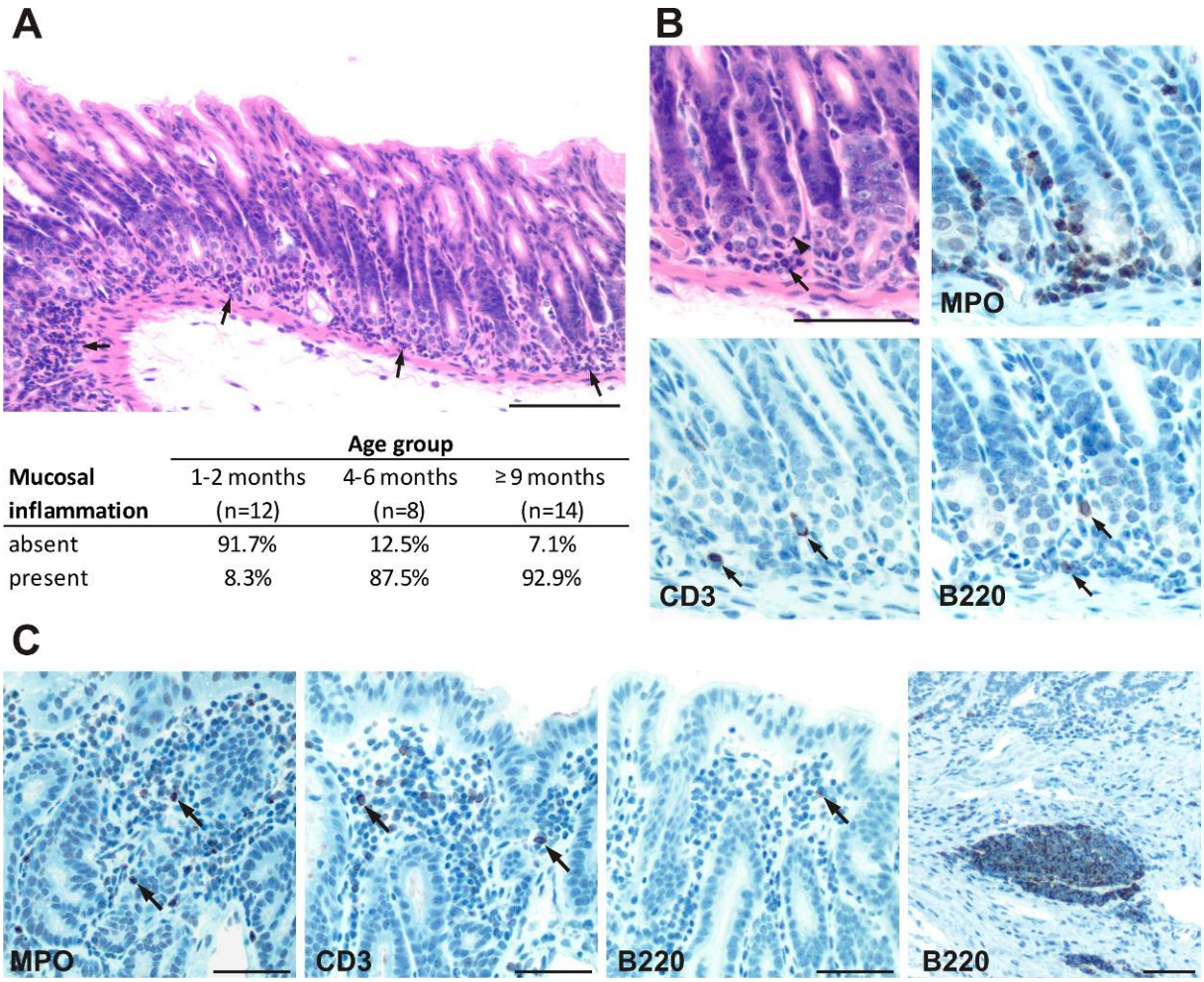

Mucosal inflammation	Age group 1-2 months (n=12)	4-6 months (n=8)	≥ 9 months (n=14)
absent	91.7%	12.5%	7.1%
present	8.3%	87.5%	92.9%

Figure 5

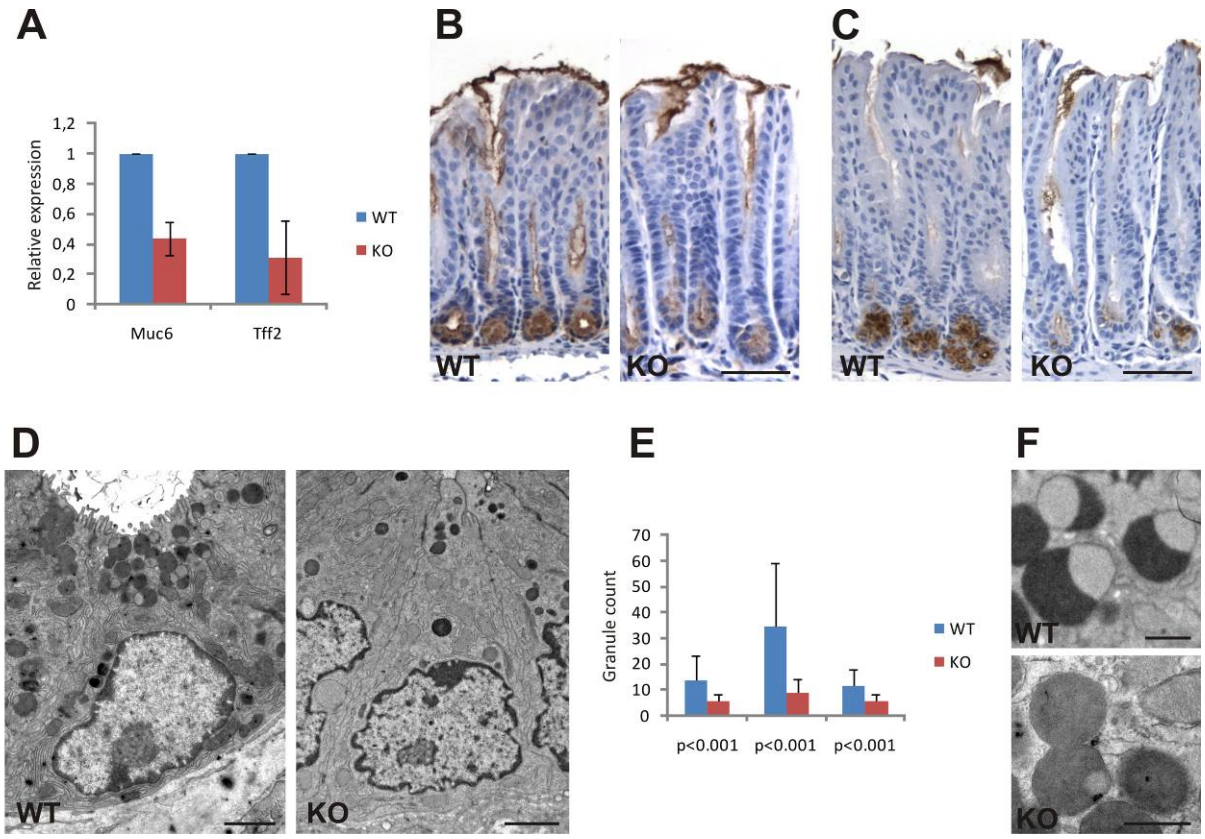

Figure 6